Semarak Engineering Journal

Journal homepage:
https://semarakilmu.com.my/journals/index.php/sem_eng/index
ISSN: 3036-0145

Magnetohydrodynamic of Williamson Hybrid Nanofluids Flow Over a Non-Linear Shrinking Sheet with Viscous Dissipation and Joule Heating

Masyfu'ah Mokhtar[1,2], Abdul Rahman Mohd Kasim[1,3,*], Iskandar Waini[4], Nur Syahidah Nordin[1,2], Siti Farah Haryatie Mohd Kanafiah[5], Adeosun Adeshina Taofeeq[1,6]

[1] Centre for Mathematical Sciences, Universiti Malaysia Pahang Al-Sultan Abdullah, Gambang, 26300 Kuantan, Pahang, Malaysia
[2] College of Computing, Informatics and Media, Universiti Teknologi MARA, Johor Branch, Segamat Campus, Johor, Segamat, 85000, Malaysia
[3] Centre for Research in Advanced Fluid and Process, University Malaysia Pahang, Lebuhraya Tun Razak, Pahang, Gambang, 26300, Malaysia
[4] Fakulti Teknologi Kejuruteraan Mekanikal dan Pembuatan, Universiti Teknikal Malaysia Melaka, Hang Tuah Jaya, Durian Tunggal 76100, Melaka, Malaysia
[5] Mathematical Sciences Studies, College of Computing, Informatics and Mathematics, Universiti Teknologi MARA (UiTM) Kelantan Branch, Machang Campus, 18500, Malaysia
[6] Federal College of Education, 232102 Iwo, Nigeria

ARTICLE INFO

Article history:
Received 30 August 2024
Received in revised form 2 October 2024
Accepted 10 November 2024
Available online 15 December 2024

Keywords:
Williamson; MHD; viscous dissipation; Joule heating; hybrid nanofluid; shrinking; bvp4c

ABSTRACT

Heat transfer plays a crucial role in various industrial applications. Thus, this study investigates the heat transfer characteristics of a non-Newtonian Williamson hybrid nanofluids flowing over a non-linear shrinking sheet, incorporating MHD effects and viscous dissipation. Alumina and Copper nanoparticles are dispersed in a CMC-water base fluid, representing a non-Newtonian hybrid nanofluid with shear thinning behaviour. The complex mathematical model is transformed into similarity equations using appropriate transformations, and the MATLAB function bvp4c is employed to solve these equations numerically. The model's accuracy is validated by comparison with an established model, demonstrating reasonable agreement. The study analyses the impact of various fluid parameters, including magnetic, Eckert number, Williamson, suction, and nanoparticle volume fraction, on fluid flow behaviour. Results show that increased suction enhances both the skin friction coefficient and heat transfer rate, while a higher Williamson parameter reduces both. The heat transfer rate decreases with an increase in the Eckert number. Additionally, an increase in the magnetic parameter and nanoparticle volume fraction leads to higher skin friction but a lower heat transfer rate.

1. Introduction

In the industrial process and manufacturing, the use of an effective working fluid is essential for achieving optimal production efficiency. In 1995, a breakthrough occurred with the introduction of Nanofluids (NFs) which consist of nanoparticles dispersed in a base fluid, as developed by Choi and Eastman [1]. These NFs have demonstrated superior performance compared to traditional fluids in

* *Corresponding author.*
E-mail address: rahmanmohd@umpsa.edu.my

https://doi.org/10.37934/sej.7.1.3147

various heat transfer applications, particularly in energy-intensive systems. Common base fluids include water and oil, while frequently used nanoparticles, such as Alumina (Al_2O_3) and Copper (Cu), are valued for their stability and high thermal conductivity, respectively. Numerous studies have been conducted to investigate the behavior of NFs [2-7], with recent research highlighting that factors such as nanoparticle type, concentration, and base fluid selection significantly enhance heat transfer rates [8].

The development of hybrid nanofluids (HNFs), achieved by adding a second type of nanoparticle to conventional NFs, has further improved their thermal properties. Pioneering experimental studies in this field include those by Turcu *et al.,* [9], Jana *et al.,* [10], and Suresh *et al.,* [11]. Since experimental work involves material preparation, which needs high financial support and even involves certain procedures which may harm humans and the environment, several researchers look for numerical approaches to overcome these challenges. Notable contributions in this area include those by Devi and Devi [12], Takabi and Salehi [13], and Xue *et al.,* [14] who developed different thermophysical correlations by implementing the Tiwari Das model of NFs to explore the heat transfer characteristics of HNFs numerically. These correlations have since been widely used to study HNFs' flow behavior over various geometries and under different conditions [15-27].

Depending on nanoparticle volume fractions and the type of base fluid, HNFs may exhibit non-Newtonian behavior characterized by complex rheological properties. Traditional Navier-Stokes equations are often inadequate for modeling such fluids, which can exhibit shear-thinning or shear-thickening behavior. In this respect, various non-Newtonian models have been employed in HNFs studies, including Casson, Maxwell, Viscoelastic, Reiner-Philippoff, and Williamson models [28-32].

Among these, the Williamson model is particularly noteworthy as it effectively represents pseudoplastic fluids, which are the most encountered non-Newtonian fluid [33]. Pseudoplastic fluids, such as polymer solutions, paint, blood, and plasma, are shear-thinning whose viscosity decreases with increasing shear stress. The Williamson model accounts for both the minimum and maximum viscosities of pseudoplastic fluids, providing more accurate results and fitting experimental data effectively [34]. Consequently, many recent studies have incorporated the mathematical formulation of HNFs with the Williamson fluid model, resulting in what is known as the Williamson hybrid nanofluids (WHNFs) model, particularly for investigating fluids with shear-thinning characteristics [32,35-38]. Most previous WHNFs studies focused on fluid flow induced by a linear velocity. However, as emphasized by Timol [39], for non-Newtonian fluids, a non-linear velocity in the form of a power law ($x^{1/3}$) should be adopted. This power law form of velocity has been explored in several studies [24, 40-43].

In the field of fluid mechanics, Crane [44] and Wang [45] were pioneers in describing the flow behavior over stretching and shrinking surfaces, respectively. These surfaces have drawn significant attention from scholars due to their diverse and important applications in technology and industry, such as wire drawing, aerodynamic extrusion of plastic sheets, hot rolling, and metal spinning. Miklavčič and Wang [46] later revealed that fluid flow solutions over a shrinking sheet are not unique. Multiple solutions have also been identified in various types of fluid flows over shrinking surfaces, including HNFs [47-49], Williamson fluid [50] and Williamson fluid with nanoparticles [51,52].

The application of magnetohydrodynamics (MHD) to fluid flow has gained importance in various fields, including nuclear reactors, plasma confinement, and metallurgical processes. MHD governs the behaviour of electrically conducting fluids in the presence of a magnetic field, where Lorentz forces influence velocity profiles and heat transfer. Considering its wide-ranging applications, numerous researchers have studied MHD HNFs [16,18,40,53-60] and MHD Williamson fluids [61,62] for various geometries and flow conditions. Kavya *et al.,* [37], Almaneea [63], Yahya *et al.,* [64], and Alkasasbeh *et al.,* [65], investigated WHNFs involving MHD effects but with different geometries,

nanoparticles and base fluids. Kavya *et al.,* [37] studied magnetic hybrid nanoparticles in a water suspension of MoS_4 and Cu nanoparticles for flow over stretching/shrinking cylinder. Almaneea [63], explored MHD HNFs composed of Al_2O_3 and Cu nanoparticles with glycerine as the base fluid for flow over a heated pipe. Kavya *et al.,* [37], and Almaneea [63] reported that as the magnetic field strength increased, the velocity profile decreased while the temperature increased. This finding consistent with Shateyi *et al.,* [61], and Hussain *et al.,* [62]. In contrast, Khashi'ie *et al.,* [40] observed the opposite trend, where the velocity increased, and the temperature decreased with an increasing magnetic parameter. Yahya *et al.,* [64] analysed the thermal performance of an engine oil-based HNF consists of Go and AA7072 nanoparticles, across a Riga wedge, while Alkasasbeh *et al.,* [65] investigated MHD WHNFs composed of SWCNTS and MWCNTS with water as the base fluid over an exponentially shrinking sheet. Recently, Ali *et al.,* [66] studied an MHD Cross ternary HNF containing MoS_2, TiO_2 and Ag with CMC-water-base fluid over a stretching cylinder. CMC-water has emerged as a popular base fluid for stabilizing HNFs [67]. Experimental results show that CMC-water exhibits shear thinning behavior, and the outcomes align well with the power-law model for non-Newtonian fluids. Recent research on MHD WHNFs flow can be found in the work of Jain *et al.,* [68], and Aselebe *et al.,* [69] focusing on viscous dissipation and Joule heating effects, respectively. These effects are particularly intriguing due to their significant impact on MHD fluid flow. Jain *et al.,* [68] compared nanofluids such as Cuo-water, SWCNT-water, and MWCNT-water and found that hybrid carbon nanotubes demonstrated superior performance in terms of skin friction and local Nusselt number compared to SWCNT-water and MWCNT-water. Meanwhile, Aselebe *et al.,* [69] reported an increase in fluid temperature due to viscous dissipation.

From the literature, there is limited research on MHD WHNFs under the combined influences of viscous dissipation and Joule heating over a shrinking sheet induced by a non-linear velocity. This study, therefore, investigates the behaviour of MHD WHNFs flow over a non-linear shrinking sheet, incorporating the effects of viscous dissipation and Joule heating. Alumina and Copper nanoparticles are suspended in a CMC-water base fluid to represent a non-Newtonian hybrid nanofluid. The existing formulation of HNFs is integrated with the Williamson fluid model. Due to the complexity of the governing equations describing fluid flow and heat transfer, the mathematical model is reduced to a simplified set of ordinary differential equations (ODEs) using a similarity transformation. These equations are then solved numerically using the bvp4c function in MATLAB. The results are presented graphically, and the effects of various fluid parameters, including the magnetic parameter, Eckert number, Williamson parameter, Prandtl number, and suction parameter, on the velocity and temperature profiles, as well as physical quantities like skin friction coefficient and Nusselt number, are analysed to elucidate fluid flow behaviour. Additionally, the simultaneous impact of the Williamson parameter and the volume fraction of nanoparticles on heat transfer enhancement is also investigated.

2. Methodology

The physical flow model of WHNFs over a shrinking sheet is illustrated in Figure 1. The surface velocity is described by $u_w\ x = ax^{1/3}$ where a is a constant and $a>0$. The parameter $v_w\ x$ represents the mass flux velocity, while $T_w\ x = T_\infty + T_0 x^{2/3}$ is treated as a variable surface temperature. Here, T_∞ and T_0 denote the ambient and constant temperatures, respectively. A magnetic field, $B(x)$, is applied transversely along the y-axis, where $B(x) = B_0 x^{-1/3}$ and B_0 represents the constant magnetic strength [40]. Additionally, the effects of viscous dissipation and Joule heating are considered in the analysis.

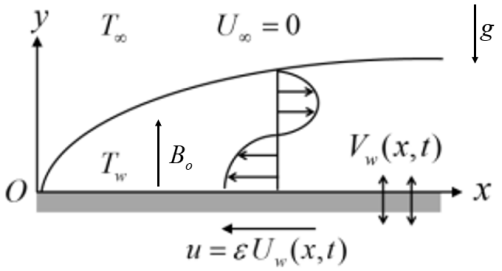

Fig. 1. Geometry of the physical problem

The governing equations for WHNFs can be derived using boundary layer approximations to the continuity, momentum, and energy equations. Consequently, the steady two-dimensional boundary layer equations for this fluid model are expressed as follows [15,24,38,70]:

$$\frac{\partial u}{\partial x}+\frac{\partial u}{\partial y}=0 \tag{1}$$

$$u\frac{\partial u}{\partial x}+v\frac{\partial u}{\partial y}=\frac{\mu_{hnf}}{\rho_{hnf}}\left(\frac{\partial^2 u}{\partial y^2}+\sqrt{2}\Gamma\frac{\partial^2 u}{\partial y^2}\frac{\partial u}{\partial y}\right)-\frac{\sigma_{hnf}}{\rho_{hnf}}B_0^2 u \tag{2}$$

$$u\frac{\partial T}{\partial x}+v\frac{\partial T}{\partial y}=\frac{k_{hnf}}{(\rho c_p)_{hnf}}\left(\frac{\partial^2 T}{\partial y^2}\right)+\frac{\mu_{hnf}}{(\rho c_p)_{hnf}}\left\{\left(\frac{\partial u}{\partial y}\right)^2+\frac{\Gamma}{\sqrt{2}}\left(\frac{\partial u}{\partial y}\right)^3\right\}+\frac{\sigma_{hnf}}{(\rho c_p)_{hnf}}B_0^2 u^2 \tag{3}$$

In this context, (x,y) represents the Cartesian coordinates, while (u,v) denote the velocity components in the x- and y-directions, respectively. Additionally, k_{hnf}, ρ_{hnf}, μ_{hnf}, $(c_p)_{hnf}$, σ_{hnf}, Γ, and g correspond to the thermal conductivity, density, dynamic viscosity, heat capacitance, electrical conductivity, time constant, and gravitational acceleration, respectively. The problem is governed by the following boundary conditions:

$$\begin{aligned} &u=\varepsilon u_w\ x\ ,\quad v=v_w\ x\ ,\quad T=T_w\ x \quad \text{at } y=0,\\ &u\to 0,\quad T\to T_\infty \quad \text{as } y\to\infty \end{aligned} \tag{4}$$

where ε represents the deformable sheet, where $\varepsilon>0$ indicates a stretching sheet, $\varepsilon<0$ denotes a shrinking sheet and $\varepsilon=0$ corresponds to a static sheet. Additionally, throughout this section, the subscripts *hnf* and *f* refer to hybrid nanofluid and regular fluid respectively.

The governing Eq. (1)-(3) are expressed as nonlinear partial differential equations (PDEs). Due to their complexity, the similarity transformation method is applied to simplify them into nonlinear ordinary differential equations (ODEs). According to references [59,68], the appropriate similarity variables are introduced in Eq. (5) as follows:

$$\eta=\frac{y}{x^{1/3}}\left(\frac{a}{\nu_f}\right)^{1/2},\quad \psi=\left(a\nu_f\right)^{1/2}x^{2/3}f(\eta),\quad \theta(\eta)=\frac{T-T_\infty}{T_w-T_\infty} \tag{5}$$

where η and θ are dimensionless similarity variables related to the stream function ψ. Utilizing these variables, and considering that $u=\frac{\partial\psi}{\partial y}$ and $v=-\frac{\partial\psi}{\partial x}$, the velocity components are transformed into:

$$u=ax^{1/3}f'\ \eta\ ,v=-\ av_f\ ^{1/2}x^{-1/3}\left(\frac{2}{3}f\ \eta\ -\frac{1}{3}\eta f'\ \eta\ \right) \tag{6}$$

which satisfied the continuity Eq. (1). Additionally, $v_w=-\ 2/3\ \ av_f\ ^{1/2}x^{-1/3}S$ represents the mass velocity at the surface, where v_f represents the fluid's kinematic viscosity and S is the suction/injection parameter. A positive S corresponds to suction, while a negative S indicates injection.

Subsequently, Eq. (5) and (6) are substituted into the governing Eq. (2) and (3) to derive the transformed ODEs, which are presented as Eq. (7) and (8):

$$\frac{\mu_{hnf}/\mu_f}{\rho_{hnf}/\rho_f}\ 1+\gamma f''\ \ f'''+\frac{2}{3}ff''-\frac{1}{3}f'^2-\frac{\sigma_{hnf}/\sigma_f}{\rho_{hnf}/\rho_f}Mf'=0 \tag{7}$$

$$\frac{1}{\mathrm{Pr}}\left(\frac{k_{hnf}}{k_f}\right)\theta''+\left(\frac{\rho c_{p\ hnf}}{\rho c_{p\ f}}\right)\left(-\frac{2}{3}f'\theta+\frac{2}{3}f\theta'\right)+\left(\frac{\mu_{hnf}}{\mu_f}\right)Ecf''^2\left\{1+\frac{\gamma}{2}f''\right\}+\left(\frac{\sigma_{hnf}}{\sigma_f}\right)EcMf'^2=0 \tag{8}$$

These equations are subject to the corresponding boundary conditions given by:

$$\begin{aligned} &f\ 0\ =S,\ f'\ 0\ =\varepsilon,\ \theta\ 0\ =1\\ &f'\ \eta\ \to 0,\ \theta\ \eta\ \to 0\ \text{as}\ \eta\to\infty \end{aligned} \tag{9}$$

In this context, the prime notation $'$ denotes differentiation with respect to η. The dimensionless parameters associated with the Williamson fluid γ, magnetic field M, Eckert number Ec, and Prandtl number Pr are defined as follows:

$$\gamma=\Gamma a\left(\frac{2a}{\nu_f}\right)^{1/2},\ M=\frac{\sigma_f\beta_0^{\ 2}}{\rho_f a},\ Ec=\frac{a^2}{T_o(c_p)_f},\ \mathrm{Pr}=\frac{\rho c_p\nu_{\ f}}{k_f}, \tag{10}$$

where $\mathrm{Re}_x=u_w\ x\ x/\nu_f$ represents the local Reynolds number.

Eq. (11) defines the physical quantities of interest, specifically the skin friction coefficient C_f and the local Nusselt number Nu_x:

$$C_f=\frac{\mu_{hnf}}{\rho_f u_w^2}\left[\frac{\partial u}{\partial y}+\frac{\Gamma}{\sqrt{2}}\left(\frac{\partial u}{\partial y}\right)^2\right]_{y=0},\ Nu_x=-\frac{xk_{hnf}}{k_f\ \ T_w-T_\infty}\left(\frac{\partial T}{\partial y}\right)_{y=0} \tag{11}$$

By substituting the variables from Eq. (5) into Eq. (11), it transforms into:

$$\mathrm{Re}_x^{1/2} C_f = \frac{\mu_{hnf}}{\mu_f} f''(0)\left(1+\frac{\gamma}{2} f''(0)\right),\ \mathrm{Re}_x^{-1/2} Nu_x = -\frac{k_{hnf}}{k_f}\theta'(0) \tag{12}$$

In this study, the thermophysical correlations used to solve the HNFs flow problem are based on the model of Takabi and Salehi [13]. For clarity, the thermophysical correlations for both NFs and HNFs are detailed in Table 1. Throughout the analysis, a volume fraction of nanoparticles $\phi_1 = \phi_2 = 0.01$ is applied, resulting in Cu-Al_2O_3/CMC-water hybrid nanofluid. Note that, ϕ_1 and ϕ_2 represent the nanoparticles concentration for Al_2O_3 and Cu, respectively, and the summation of them represented by ϕ_{hnf}. Additionally, the thermophysical properties of the base fluid (CMC-water) and the nanoparticles (Cu, and Al_2O_3) are listed in Table 2 [71,72].

Table 1
Thermophysical properties for nanofluid and hybrid nanofluid

Element	Nanofluid	Hybrid nanofluid
Viscosity	$\frac{\mu_{nf}}{\mu_f} = \frac{1}{(1-\phi)^{2.5}}$	$\frac{\mu_{hnf}}{\mu_f} = \frac{1}{(1-\phi_{hnf})^{2.5}}$
Density	$\rho_{nf} = (1-\phi)\rho_f + \phi\rho_s$	$\rho_{hnf} = (1-\phi_{hnf})\rho_f + \phi_1\rho_{s1} + \phi_2\rho_{s2}$
Heat capacity	$(\rho C_p)_{nf} = (1-\phi)(\rho C_p)_f + \phi(\rho C_p)_s$	$(\rho C_p)_{hnf} = (1-\phi_{hnf})(\rho C_p)_f + \phi_1(\rho C_p)_{s1} + \phi_2(\rho C_p)_{s2}$
Thermal conductivity	$\frac{k_{nf}}{k_f} = \frac{k_s + 2k_f - 2\phi(k_f - k_s)}{k_s + 2k_f + \phi(k_f - k_s)}$	$\frac{k_{hnf}}{k_f} = \frac{\left(\frac{\phi_1 k_{s1} + \phi_2 k_{s2}}{\phi_{hnf}}\right) + 2k_{bf} + 2(\phi_1 k_{s1} + \phi_2 k_{s2}) - 2\phi_{hnf} k_{bf}}{\left(\frac{\phi_1 k_{s1} + \phi_2 k_{s2}}{\phi_{hnf}}\right) + 2k_{bf} - (\phi_1 k_{s1} + \phi_2 k_{s2}) + \phi_{hnf} k_{bf}}$
Electrical conductivity	$\frac{\sigma_{nf}}{\sigma_f} = \frac{\sigma_s + 2\sigma_f - 2\phi(\sigma_f - \sigma_s)}{\sigma_s + 2\sigma_f + \phi(\sigma_f - \sigma_s)}$	$\frac{\sigma_{hnf}}{\sigma_f} = \frac{\left(\frac{\phi_1\sigma_{s1} + \phi_2\sigma_{s2}}{\phi_{hnf}}\right) + 2\sigma_{bf} + 2(\phi_1\sigma_{s1} + \phi_2\sigma_{s2}) - 2\phi_{hnf}\sigma_{bf}}{\left(\frac{\phi_1\sigma_{s1} + \phi_2\sigma_{s2}}{\phi_{hnf}}\right) + 2\sigma_{bf} - (\phi_1\sigma_{s1} + \phi_2\sigma_{s2}) + \phi_{hnf}\sigma_{bf}}$
		where $\phi_{hnf} = \phi_1 + \phi_2$

Table 2
Thermophysical properties for the base fluid and nanoparticles

Thermophysical properties	Base fluid	Nano particle	
	CMC-water	Al_2O_3	Cu
Density, $\rho(kg/m^3)$	997.1	3970	8933
Heat capacitance, $C_p(J/kgK)$	4179	765	385
Thermal conductivity, $k(W/mK)$	0.613	40	400
Electrical conductivity, $\sigma(S/m)$	0.05	0.85	1.67
Prandtl, Pr	6.2		

3. Results

Eq. (7) to (9) were solved using the numerical approach with MATLAB's bvp4c function. The effects of various physical parameters on the WHNFs flow behavior were analyzed by adjusting the control parameters accordingly. Prior to obtaining the solutions, a validation process was carried out to ensure the accuracy of the current model. Under specific limiting conditions, the momentum equation in this study was reduced to those found in previous works by Waini *et al.,* [24], Cortell [41], and Ferdows *et al.,* [42], as shown in Table 3. The accuracy of the current numerical method was

confirmed when the values of $f''(0)$, as presented in Table 4, showed reasonable agreement with previous studies. These values were obtained under the condition of a stretching sheet $\varepsilon = 1$ for various values of S and certain limiting values.

Table 3
Comparative model in terms of momentum equations

Author	Model	Limiting cases
Current	$\frac{\left(\mu_{hnf}/\mu_f\right)}{\left(\rho_{hnf}/\rho_f\right)} f'''\left(1+\gamma f''\right)+\frac{2}{3} ff''-\frac{1}{3} f'^2-\frac{\sigma_{hnf}/\sigma_f}{\rho_{hnf}/\rho_f} Mf'=0$	$\gamma = M = \phi_{hnf} = 0$
Waini *et al.,* [24]	$3\frac{\mu_{hnf}/\mu_f}{\rho_{hnf}/\rho_f} f'''+2ff''-f'^2=0$	
Cortell [41]	$3f'''+2ff''-\left(f'\right)^2=0$	
Ferdows *et al.,* [42]	$f'''+\frac{2}{3} ff''-\frac{1}{3}\left(f'^2-Mf'^2\right)+Gr\theta+Gc\phi=0$	$M = Gr = Gc = 0$

Table 4
Comparative values of $f''(0)$ for various values of S when $\Pr = 2$, $\gamma = M = \phi_{hnf} = 0$, and $\varepsilon = 1$

S	Cortel [41]	Ferdows *et al.,* [42]	Waini *et al.,* [24]	Current
0.75	-0.453521	-0.453523	-0.453523	-0.453526660
-0.5	-0.518869	-0.518869	-0.518869	-0.518871662
0	-0.677647	-0.677648	-0.677648	-0.677648605
0.5	-0.873627	-0.873643	-0.873643	-0.873642953
0.75	-0.984417	-0.984439	-0.984439	-0.984439416

The fluid flow of HNFs is characterized by 2% nanoparticle concentration $\phi_1 = \phi_2 = 0.01$ and is driven by a shrinking surface $\varepsilon = -1$. The solutions for the skin friction coefficient, $\mathrm{Re}_x^{1/2} C_f$ and the Nusselt number, $\mathrm{Re}_x^{-1/2} Nu_x$ for various parameter values are recorded in Table 5. An increase in the values of S enhances both $\mathrm{Re}_x^{1/2} C_f$ and $\mathrm{Re}_x^{-1/2} Nu_x$. In contrast, increasing the values of γ results in a decrease in these physical quantities. Additionally, the values of $\mathrm{Re}_x^{1/2} C_f$ and $\mathrm{Re}_x^{-1/2} Nu_x$ increase and decrease, respectively, with the rise of M. Moreover, Ec and $\Pr$ have no effect on $\mathrm{Re}_x^{1/2} C_f$. However, these parameters influence the energy equation. As a result, the values of $\mathrm{Re}_x^{-1/2} Nu_x$ are affected, decreasing as Ec increase but increasing as $\Pr$ rise. Physically, the presence of suction and a higher Prandtl number tends to release energy to the flow, while the Williamson fluid parameter, magnetic parameter, and Eckert number act to hinder the flow's energy.

Table 5
Values of $\mathrm{Re}_x^{1/2} C_f$ and $\mathrm{Re}_x^{-1/2} Nu_x$ for different physical parameters when $\varepsilon = -1$, $\phi_1 = \phi_2 = 0.01$.

S	γ	M	Ec	$\Pr$	$\mathrm{Re}_x^{1/2} C_f$	$\mathrm{Re}_x^{-1/2} Nu_x$
2.25	0.01	0.01	0.1	6.2	1.110990647	7.822658227
2.24					1.092462312	7.776725260
2.22					1.050075988	7.683979925
2.25	0.02				1.106574516	7.821477794
	0.03				1.102116671	7.820313237
	0.04				1.097612236	7.819163763

	0.01	0			1.080725411	7.830468736
		0.02			1.136413715	7.815525959
		0.03			1.158831679	7.808865051
		0.01	0		1.110990649	8.289691565
			0.2		1.110990647	7.355624890
			0.3		1.110990647	6.888591552
			0.1	7	1.110990649	8.958907313
				8	1.110990649	10.378906129
				10	1.110990667	13.217952059

The velocity $f'\ \eta$ and temperature $\theta\ \eta$ profiles for the previously mentioned parameters are shown in Figures 2-9. The far-field boundary conditions were satisfied asymptotically. Figures 2 and 3 illustrate the effect of magnetic parameters M on the velocity $f'\ \eta$ and temperature profile $\theta\ \eta$. It is observed that as this parameter increases, the velocity increases, whereas the temperature decreases along the shrinking surface. Theoretically, magnetic parameters may reduce the velocity due to the Lorentz force, but in the present study, the velocity increases. Figures 4 and 5 depict the influence of the Eckert number, Ec and the Prandtl number, Pr on the temperature profile $\theta\ \eta$, respectively. Both parameters lead to an increase in the temperature profile $\theta\ \eta$.

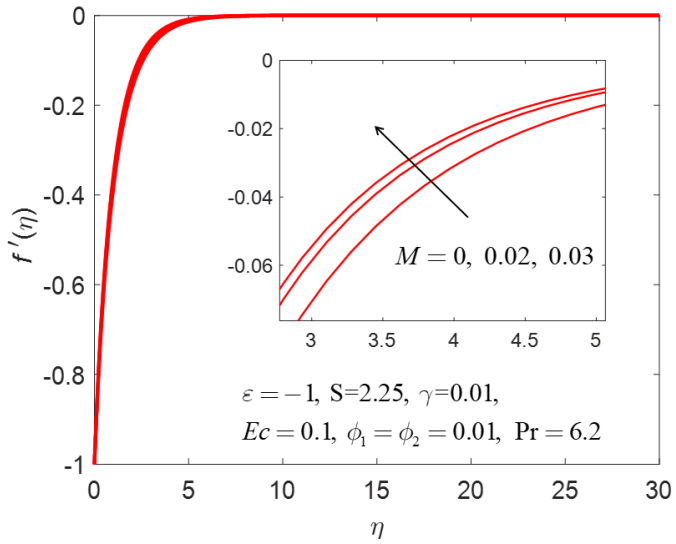

Fig. 2. $f'\ \eta$ for different values of M

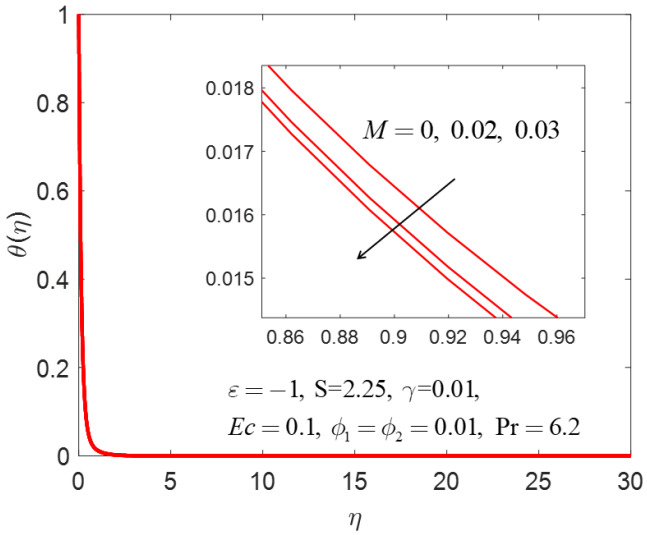

Fig. 3. $\theta\ \eta$ for different values of M

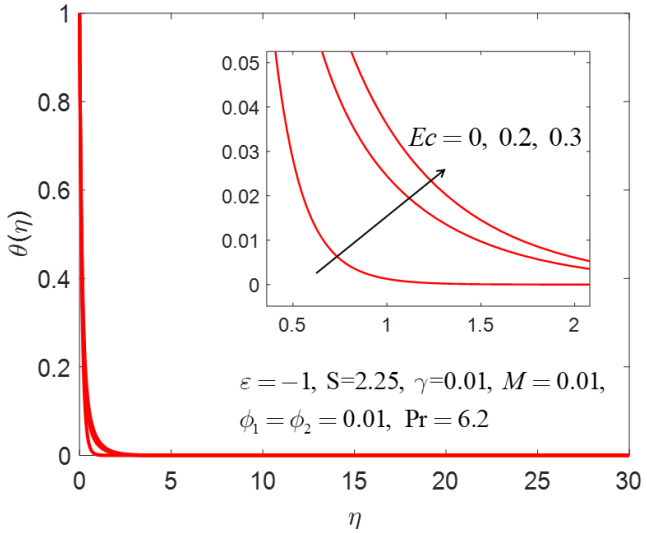

Fig. 4. $\theta\ \eta$ for different values of Ec

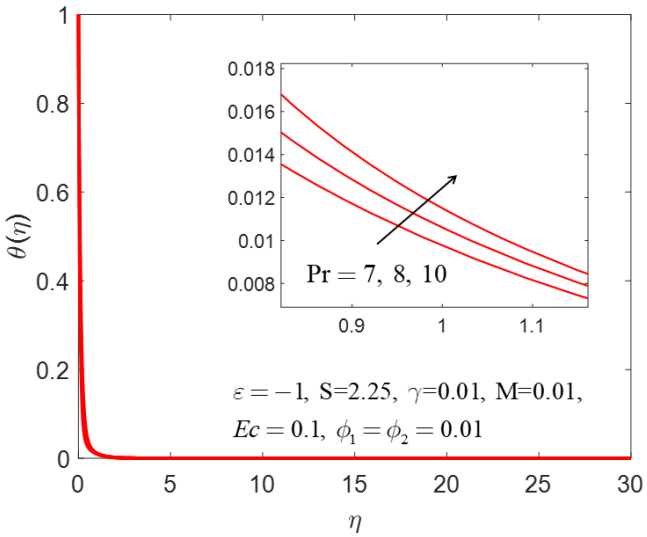

Fig. 5. $f'\ \eta$ for different values of Pr

Figures 6 and 7 illustrate the effects of the Williamson number γ on velocity $f'\eta$ and temperature $\theta\ \eta$, respectively. It is observed that as γ increases, the fluid's velocity decreases while the temperature increases. Since the Williamson number represents the ratio of relaxation time to specific process time, a decrease in specific process time leads to a higher Williamson number. As a result, both velocity and boundary layer thickness are reduced. Physically, the Williamson parameter enhances the non-Newtonian behavior of the fluid by increasing its resistance due to frictional effects. Consequently, the fluid slows down, allowing more time for heat absorption from the surface, which raises the temperature.

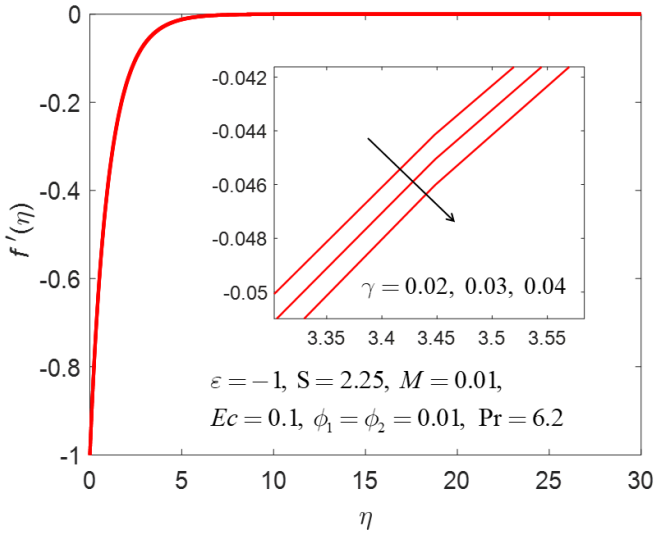

Fig. 6. $f'\ \eta$ for different values of γ

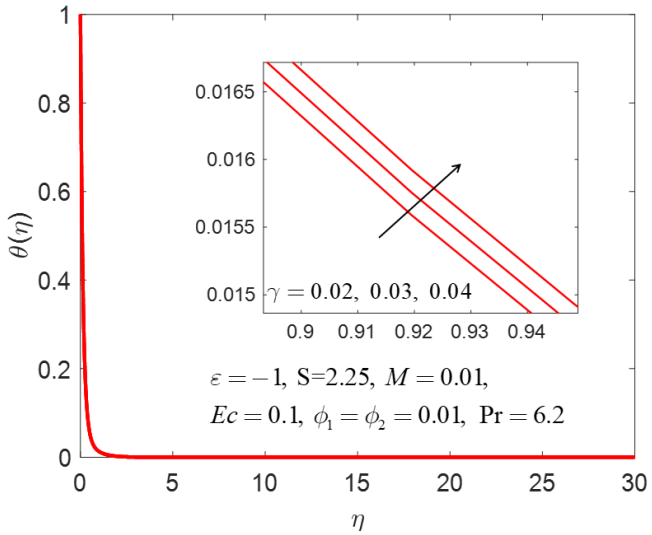

Fig. 7. $\theta\ \eta$ for different values of γ

Figures 8 and 9 show the effects of the suction parameter S on velocity $f'\ \eta$ and temperature $\theta\ \eta$, respectively. It is observed that the velocity increases due to mass transfer at the suction wall, while the temperature decreases. Physically, as the suction strength in the flow increases, the velocity increases because the decelerated fluid particles are removed at the surface. As a result, heat is dissipated more quickly, leading to a decrease in the fluid temperature.

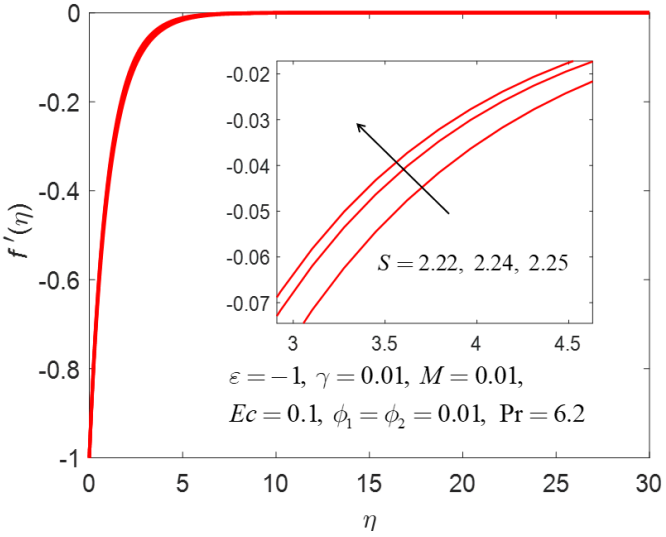

Fig. 8. $f'\ \eta$ for different values of S

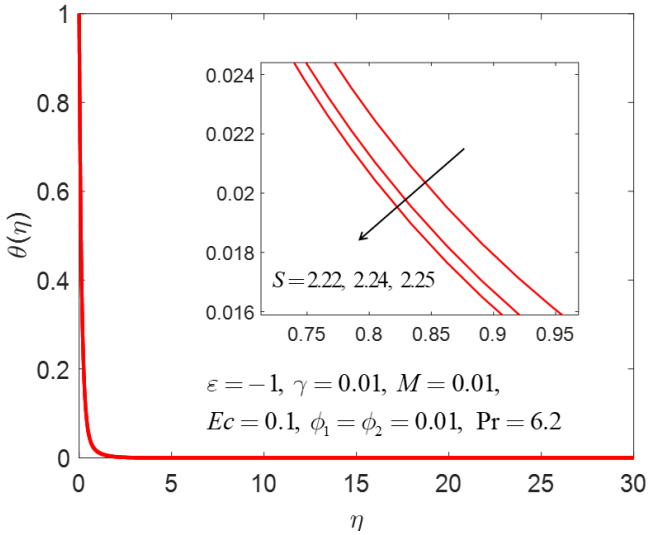

Fig. 9. $\theta\ \eta$ for different values of S

The combined effects of the Williamson parameter γ and the volume fraction of nanoparticles ϕ_1, ϕ_2 on $\mathrm{Re}_x^{1/2} C_f$ and $\mathrm{Re}_x^{-1/2} Nu_x$ are shown in Table 6 and 7, respectively. It is observed that the values of $\mathrm{Re}_x^{1/2} C_f$ gradually decrease by 1.47% when γ increases from 0 to 0.03 for the case of $\phi_1 = \phi_2 = 0.01$. However, the values of $\mathrm{Re}_x^{-1/2} Nu_x$ are only slightly affected by γ, with a 0.05% decrease. For the case of $\gamma = 0$, the values of $\mathrm{Re}_x^{1/2} C_f$ are significantly increased by 23.70% when the concentration of Cu increases from 0.5% to 2% in the base fluid. However, the values of $\mathrm{Re}_x^{-1/2} Nu_x$ slightly decreased by 0.47%.

Table 6
Values of $\mathrm{Re}_x^{1/2} C_f$ when, $\varepsilon = -1, \gamma = 0.01, M = Ec = 0, S = 2.25, \Pr = 6.2$

γ	$\phi_1 = 0.01, = \phi_2 = 0.005$	$\phi_1 = 0.01, = \phi_2 = 0.01$	$\phi_1 = 0.01, = \phi_2 = 0.02$
0	0.994175254	1.085933948	1.229762975
0.01	0.985719569	1.080725376	1.225628600
0.02	0.976215875	1.075414429	1.221485537
0.03	0.964932440	1.069986681	1.217331669

Table 7
Values of $\mathrm{Re}_x^{-1/2} Nu_x$ when, $\varepsilon = -1, \gamma = 0.01, M = Ec = 0, S = 2.25, \mathrm{Pr} = 6.2$

γ	$\phi_1 = 0.01, = \phi_2 = 0.005$	$\phi_1 = 0.01, = \phi_2 = 0.01$	$\phi_1 = 0.01, = \phi_2 = 0.02$
0	8.297562702	8.286588416	8.258380193
0.01	8.295658524	8.285119660	8.256933084
0.02	8.293605242	8.283651914	8.255503825
0.03	8.291286325	8.282182473	8.254091418

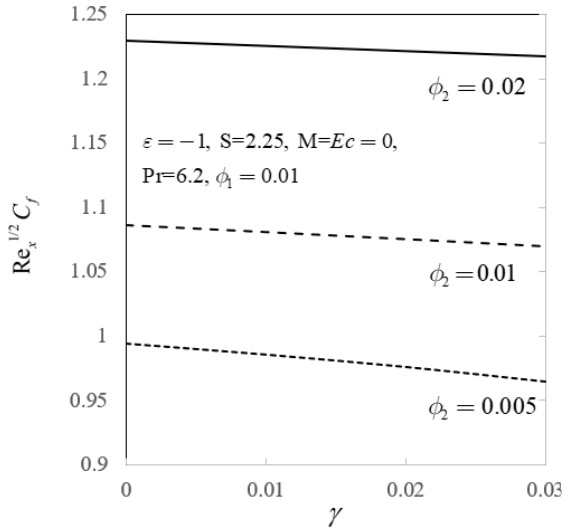

Fig. 10. Variation of $\mathrm{Re}_x^{1/2} C_f$ against γ for different values of ϕ_2

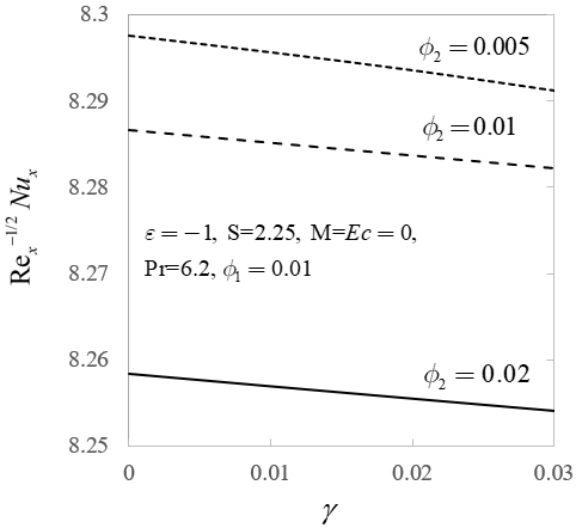

Fig. 11. Variation of $\mathrm{Re}_x^{-1/2} Nu_x$ against γ for different values of ϕ_2

To gain more insight, Figures 10 and 11 are presented to demonstrate the simultaneous effects of the Williamson parameter γ and various nanoparticle concentrations ϕ_1, ϕ_2 on $\mathrm{Re}_x^{1/2} C_f$ and $\mathrm{Re}_x^{-1/2} Nu_x$, respectively. The Al_2O_3-Cu/CMC-water hybrid nanofluid $(\phi_1 = 0.01, \phi_2 = 0.02)$ with the highest nanoparticle concentration exhibits the highest skin friction but the lowest Nusselt number, followed by Al_2O_3-Cu/CMC-water hybrid nanofluid $(\phi_1 = \phi_2 = 0.01)$ with a moderate concentration, and then the Al_2O_3-Cu/CMC-water hybrid nanofluid $(\phi_1 = 0.01, \phi_2 = 0.05)$ with the lowest

concentration. Physically, an increase in nanoparticles concentration enhances the fluid's viscosity, causing the fluid to slow down and reducing heat transfer performance. Furthermore, an increase in the Williamson parameter γ significantly affects both skin friction and heat transfer rate, which is consistent with its relationship to the velocity term in Eq. (7) and the energy term in Eq. (8).

4. Conclusions

This study investigates the impact of various fluid parameters, such as the magnetic parameter, Eckert number, Williamson parameter, Prandtl number, suction parameter, and nanoparticle volume fraction, on velocity and temperature profiles, as well as physical quantities like skin friction and the heat transfer rate. The results indicate that an increase in the Williamson parameter leads to a decrease in velocity but an increase in temperature. In contrast, higher values of the magnetic and suction parameters result in increased velocity but decreased temperature. It was also observed that suction allows the WHNFs molecules to gain control of the surface, enhancing the heat transfer rate. Meanwhile, a higher Williamson parameter reduces both skin friction and heat transfer rate due to the obstacles that appear by the shear-thinning phenomenon, which diminishes fluid interaction with surfaces and generates less drag force. The heat transfer rate decreases with an increase in the Eckert number and increases with a rise in the Prandtl Number in the operating fluid. Moreover, an increase in magnetic parameters and nanoparticle volume fraction results in higher skin friction but a lower heat transfer rate.

The present findings are only conclusive to the non-linear shrinking sheet. Theoretically, magnetic parameters and nanoparticles enhance the heat transfer rate. However, in this study, the higher suction strength may influence the heat transfer process. Thus, this study will be a reference for future research to further study and investigate the other physical parameters or hybrid nanomaterials that may enhance the heat transfer rate, particularly for the shrinking sheet case.

Acknowledgement

The authors sincerely acknowledge Universiti Malaysia Pahang Al-Sultan Abdullah for the financial support provided under research grant PGRS2303145. Appreciation is also extended to Universiti Teknologi MARA (UiTM) Johor Branch, Universiti Teknologi MARA (UiTM) Kelantan Branch, Universiti Teknikal Malaysia Melaka, and the Federal College of Education, Nigeria, for their invaluable guidance and support.

References

[1] Choi, S. US, and Jeffrey A. Eastman. *Enhancing thermal conductivity of fluids with nanoparticles*. No. ANL/MSD/CP-84938; CONF-951135-29. Argonne National Lab.(ANL), Argonne, IL (United States), 1995.

[2] Khanafer, Khalil, Kambiz Vafai, and Marilyn Lightstone. "Buoyancy-driven heat transfer enhancement in a two-dimensional enclosure utilizing nanofluids." *International journal of heat and mass transfer* 46, no. 19 (2003): 3639-3653. https://doi.org/10.1016/S0017-9310(03)00156-X

[3] Tiwari, Raj Kamal, and Manab Kumar Das. "Heat transfer augmentation in a two-sided lid-driven differentially heated square cavity utilizing nanofluids." *International Journal of heat and Mass transfer* 50, no. 9-10 (2007): 2002-2018. https://doi.org/10.1016/j.ijheatmasstransfer.2006.10.010

[4] Oztop, Hakan F., and Eiyad Abu-Nada. "Numerical study of natural convection in partially heated rectangular enclosures filled with nanofluids." *International journal of heat and fluid flow* 29, no. 5 (2008): 1326-1336. https://doi.org/10.1016/j.ijheatfluidflow.2008.02.004

[5] Bachok, Norfifah, Anuar Ishak, and Ioan Pop. "Stagnation-point flow over a stretching." *Nanoscale research letters* 6, no. 1 (2011): 1-10. https://doi.org/10.1186/1556-276X-6-623

[6] Yacob, Nor Azizah, Anuar Ishak, Ioan Pop, and Kuppalapalle Vajravelu. "Boundary layer flow past a stretching/shrinking surface beneath an external uniform shear flow with a convective surface boundary condition in a nanofluid." *Nanoscale research letters* 6 (2011): 1-7. https://doi.org/10.1186/1556-276X-6-314

[7] Waini, Iskandar, Anuar Ishak, and Ioan Pop. "Dufour and Soret effects on Al2O3-water nanofluid flow over a moving thin needle: Tiwari and Das model." *International Journal of Numerical Methods for Heat & Fluid Flow* 31, no. 3 (2021): 766-782. https://doi.org/10.1108/HFF-03-2020-0177

[8] Kumar, Sunil, Mridul Sharma, Anju Bala, Anil Kumar, Rajesh Maithani, Sachin Sharma, Tabish Alam, Naveen Kumar Gupta, and Mohsen Sharifpur. "Enhanced heat transfer using oil-based nanofluid flow through Conduits: A Review." *Energies* 15, no. 22 (2022): 8422. https://doi.org/10.3390/en15228422

[9] Turcu, R., A. L. Darabont, A. Nan, N. Aldea, D. Macovei, D. Bica, L. Vekas et al. "New polypyrrole-multiwall carbon nanotubes hybrid materials." *Journal of optoelectronics and advanced materials* 8, no. 2 (2006): 643-647.

[10] Jana, S., A. Salehi-Khojin, dan W. H. Zhong. "Enhancement of Fluid Thermal Conductivity by the Addition of Single and Hybrid Nano-Additives." *Thermochimica Acta* 462 (2007): 45–55. https://doi.org/10.1016/j.tca.2007.01.032

[11] Suresh, S., K. P. Venkitaraj, P. Selvakumar, dan M. Chandrasekar. "Synthesis of Al_2O_3-Cu/Water Hybrid Nanofluids Using Two-Step Method and Its Thermo-Physical Properties." *Colloids and Surfaces A: Physicochemical and Engineering Aspects* 388 (2011): 41–48. https://doi.org/10.1016/j.colsurfa.2011.08.005

[12] Devi, S. A., dan S. S. U. Devi. "Numerical Investigation of Hydromagnetic Hybrid Cu–Al_2O_3/Water Nanofluid Flow over a Permeable Stretching Sheet with Suction." *International Journal of Nonlinear Sciences and Numerical Simulation* 17, no. 5 (2016): 249–57. https://doi.org/10.1515/ijnsns-2016-0037

[13] Takabi, B., dan S. Salehi. "Augmentation of the Heat Transfer Performance of a Sinusoidal Corrugated Enclosure by Employing Hybrid Nanofluid." *Advances in Mechanical Engineering* 6 (2014): 147059. https://doi.org/10.1155/2014/147059

[14] Xue, Q. Z. "Model for Thermal Conductivity of Carbon Nanotube-Based Composites." *Physica B: Condensed Matter* 368, no. 1–4 (2005): 302–7. https://doi.org/10.3390/en15228422

[15] Megahed, A. "Williamson Fluid Flow Due to a Nonlinearly Stretching Sheet with Viscous Dissipation and Thermal Radiation." *Journal of the Egyptian Mathematical Society* 27, no. 1 (2019). https://doi.org/10.1016/j.physb.2005.06.004

[16] Khashi'ie, N. S., N. M. Arifin, R. Nazar, E. H. Hafidzuddin, N. Wahi, dan I. Pop. "Magnetohydrodynamics (MHD) Axisymmetric Flow and Heat Transfer of a Hybrid Nanofluid Past a Radially Permeable Stretching/Shrinking Sheet with Joule Heating." *Chinese Journal of Physics* 64 (April 2020): 251–63. https://doi.org/10.1016/j.cjph.2019.11.008

[17] Wahid, N. S., N. M. Arifin, M. Turkyilmazoglu, M. E. H. Hafidzuddin, dan N. A. A. Rahmin. "MHD Hybrid Cu-Al_2O_3/Water Nanofluid Flow with Thermal Radiation and Partial Slip Past a Permeable Stretching Surface: Analytical Solution." *Journal of Nano Research* 64 (2020): 75–91. https://doi.org/10.4028/www.scientific.net/JNanoR.64.75

[18] Waini, I., A. Ishak, dan I. Pop. "MHD Flow and Heat Transfer of a Hybrid Nanofluid Past a Permeable Stretching/Shrinking Wedge." *Applied Mathematics and Mechanics (English Edition)* 41, no. 3 (March 2020): 507–20. https://doi.org/10.1007/s10483-020-2584-7

[19] Waini, I., A. Ishak, dan I. Pop. "Squeezed Hybrid Nanofluid Flow over a Permeable Sensor Surface." *Mathematics* 8, no. 6 (June 2020). https://doi.org/10.3390/math8060898

[20] Khashi'ie, N. S., I. Waini, N. A. Zainal, K. Hamzah, dan A. R. Mohd Kasim. "Hybrid Nanofluid Flow Past a Shrinking Cylinder with Prescribed Surface Heat Flux." *Symmetry* 12, no. 9 (September 2020). https://doi.org/10.3390/sym12091493

[21] Khashi'ie, N. S., N. M. Arifin, N. C. Rosca, A. V. Rosca, dan I. Pop. "Three-Dimensional Flow of Radiative Hybrid Nanofluid Past a Permeable Stretching/Shrinking Sheet with Homogeneous-Heterogeneous Reaction." *International Journal of Numerical Methods for Heat & Fluid Flow* 32, no. 2 (January 2022): 568–88. https://doi.org/10.1108/HFF-01-2021-0017

[22] Khashi'ie, N. S., I. Waini, A. Ishak, dan I. Pop. "Blasius Flow Over a Permeable Moving Flat Plate Containing Cu-Al_2O_3 Hybrid Nanoparticles with Viscous Dissipation and Radiative Heat Transfer." *Mathematics* 10, no. 8 (April 2022). https://doi.org/10.3390/math10081281

[23] Wahid, N. S., N. M. Arifin, N. S. Khashi'ie, I. Pop, N. Bachok, dan M. E. H. Hafidzuddin. "Flow and Heat Transfer of Hybrid Nanofluid Induced by an Exponentially Stretching/Shrinking Curved Surface." *Case Studies in Thermal Engineering* 25 (June 2021). https://doi.org/10.1016/j.csite.2021.100986

[24] Waini, I., A. Ishak, dan I. Pop. "Hybrid Nanofluid Flow and Heat Transfer Over a Nonlinear Permeable Stretching/Shrinking Surface." *International Journal of Numerical Methods for Heat & Fluid Flow* 29, no. 9 (2019): 3110–27. https://doi.org/10.1108/HFF-01-2019-0057

[25] Khashi'ie, N. S., I. Waini, S. M. Zokri, A. R. M. Kasim, N. M. Arifin, dan I. Pop. "Stagnation Point Flow of a Second-Grade Hybrid Nanofluid Induced by a Riga Plate." *International Journal of Numerical Methods for Heat & Fluid Flow* 32, no. 7 (2022): 2221–39. https://doi.org/10.1108/HFF-08-2021-0534

[26] Asghar, A., dan Y. Y. Teh. "Three-Dimensional MHD Hybrid Nanofluid Flow with Rotating Stretching/Shrinking Sheet and Joule Heating." *CFD Letters* 13, no. 8 (2021). https://doi.org/10.37934/cfdl.13.8.119

[27] Anuar, N. S., N. Bachok, N. M. Arifin, dan H. Rosali. "Effect of Suction/Injection on Stagnation Point Flow of Hybrid Nanofluid Over an Exponentially Shrinking Sheet with Stability Analysis." *CFD Letters* 11, no. 12 (2019): 21–33. https://doi.org/10.3390/sym11040522
[28] Gul, T., S. Mukhtar, W. Alghamdi, Z. Raizah, S. E. Alhazmi, dan E. T. ElDin. "Radiative Couple Stress Casson Hybrid Nanofluid Flow Over an Inclined Stretching Surface Due to Nonlinear Convection and Slip Boundaries." *Frontiers in Energy Research* 10 (2022). https://doi.org/10.3389/fenrg.2022.965309
[29] Gul, T., S. Mukhtar, W. Alghamdi, E. T. Eldin, M. F. Yassen, dan K. Guedri. "The Radiative Flow of the Thin-Film Maxwell Hybrid Nanofluids on an Inclined Plane in a Porous Space." *Frontiers in Energy Research* 10 (2022). https://doi.org/10.3389/fenrg.2022.970293
[30] Gul, T., S. Mukhtar, W. Alghamdi, I. Ali, A. Saeed, dan P. Kumam. "Entropy and Bejan Number Influence on the Liquid Film Flow of Viscoelastic Hybrid Nanofluids in a Porous Space in Terms of Heat Transfer." *ACS Omega* 7, no. 37 (2022): 33365–74. https://doi.org/10.1021/acsomega.2c03975
[31] Nordin, N. S., H. A. M. Al-Sharifi, A. R. M. Kasim, I. Waini, M. Mokhtar, M. F. Romlie, D. Samsudin, dan D. Adytia. "Mathematical Model of Reiner-Philippoff Embedded with Al_2O_3 and Cu Particles Over a Shrinking Sheet with Mixed Convection and Mass Flux Effect." *Journal of Advanced Research in Fluid Mechanics and Thermal Sciences* 111, no. 2 (2023): 195–213. https://doi.org/10.37934/arfmts.111.2.195213
[32] Mokhtar, M., A. R. M. Kasim, I. Waini, N. S. Nordin, H. Sakidin, A. Sukri, dan D. Adytia. "Combined Convective Transport of Williamson Hybrid Nanofluid Over a Shrinking Sheet." *Journal of Advanced Research in Fluid Mechanics and Thermal Sciences* 110, no. 2 (2023): 219–35. https://doi.org/10.37934/arfmts.110.2.219235
[33] Williamson, R. V. "The Flow of Pseudoplastic Materials." *Journal of Industrial & Engineering Chemistry* 21, no. 11 (1929): 1108–11. https://doi.org/10.1021/ie50259a019
[34] Nadeem, S., S. T. Hussain, dan C. Lee. "Flow of a Williamson Fluid Over a Stretching Sheet." *Brazilian Journal of Chemical Engineering* 30, no. 3 (July 2013): 619–25. https://doi.org/10.1590/S0104-66322013000300019
[35] Jamshed, W., K. S. Nisar, R. W. Ibrahim, T. Mukhtar, V. Vijayakumar, dan F. Ahmad. "Computational Framework of Cattaneo-Christov Heat Flux Effects on Engine Oil-Based Williamson Hybrid Nanofluids: A Thermal Case Study." *Case Studies in Thermal Engineering* 26 (August 2021). https://doi.org/10.1016/j.csite.2021.101179
[36] Jamshed, W., et al. "Entropy Amplified Solitary Phase Relative Probe on Engine Oil-Based Hybrid Nanofluid." *Chinese Journal of Physics* 77 (June 2022): 1654–81. https://doi.org/10.1016/j.cjph.2022.03.017
[37] Kavya, S., V. Nagendramma, N. A. Ahammad, S. Ahmad, C. S. K. Raju, dan N. A. Shah. "Magnetic-Hybrid Nanoparticles with Stretching/Shrinking Cylinder in a Suspension of MoS_4 and Copper Nanoparticles." *International Communications in Heat and Mass Transfer* 136 (July 2022). https://doi.org/10.1016/j.icheatmasstransfer.2022.106150
[38] Rosli, W. M. H. W., M. K. A. Mohamed, N. M. Sarif, N. F. Mohammad, dan S. K. Soid. "Boundary layer flow of Williamson hybrid ferrofluid over a permeable stretching sheet with thermal radiation effects." *CFD Letters* 15, no. 3 (2023): 112–22. https://doi.org/10.37934/cfdl.15.3.112122
[39] Timol, M.G., dan N.L. Kalthia. "Similarity Solutions of Three-Dimensional Boundary Layer Equations of Non-Newtonian Fluids." *International Journal of Non-Linear Mechanics* 21, no. 6 (1986): 475–81. https://doi.org/10.1016/0020-7462(86)90043-0
[40] Khashi'ie, N. S., I. Waini, A. R. M. Kasim, N. A. Zainal, A. Ishak, dan I. Pop. "Magnetohydrodynamic and Viscous Dissipation Effects on Radiative Heat Transfer of Non-Newtonian Fluid Flow Past a Nonlinearly Shrinking Sheet: Reiner–Philippoff Model." *Alexandria Engineering Journal* 61, no. 10 (2022): 7605–17. https://doi.org/10.1016/j.aej.2022.01.014
[41] Cortell, R. "Heat and Fluid Flow Due to Non-Linearly Stretching Surfaces." *Applied Mathematics and Computation* 217, no. 19 (2011): 7564–72. https://doi.org/10.1016/j.amc.2011.02.056
[42] Ferdows, M., M.J. Uddin, dan A.A. Afify. "Scaling Group Transformation for MHD Boundary Layer Free Convective Heat and Mass Transfer Flow Past a Convectively Heated Nonlinear Radiating Stretching Sheet." *International Journal of Heat and Mass Transfer* 56, no. 1-2 (2013): 181–87. https://doi.org/10.1016/j.ijheatmasstransfer.2012.09.020
[43] Waini, I., A. Ishak, dan I. Pop. "Eyring-Powell Fluid Flow Past a Shrinking Sheet: Effect of Magnetohydrodynamic (MHD) and Joule Heating." *Journal of Advanced Research in Fluid Mechanics and Thermal Sciences* 116, no. 1 (2024): 64–77. https://doi.org/10.37934/arfmts.116.1.6477
[44] Crane, L. J. "Flow Past a Stretching Plate." *Z. Angew. Math. Phys. (ZAMP)* 21 (1970): 645–47. https://doi.org/10.1007/BF01587695
[45] Wang, C. Y. "Liquid Film on an Unsteady Stretching Surface." *Quarterly of Applied Mathematics* 48, no. 4 (1990): 601–10. https://doi.org/10.1090/qam/1079908
[46] Miklavčič, M., dan C. Y. Wang. "Viscous Flow Due to a Shrinking Sheet." *Quarterly of Applied Mathematics* 64 (2006): 283–290. https://doi.org/10.1090/S0033-569X-06-01002-5

[47] Bakar, S. A., N. M. Arifin, N. S. Khashiie, dan N. Bachok. "Hybrid Nanofluid Flow Over a Permeable Shrinking Sheet Embedded in a Porous Medium with Radiation and Slip Impacts." *Mathematics* 9, no. 8 (April 2021). https://doi.org/10.3390/math9080878

[48] Lund, L. A., Z. Omar, I. Khan, A. H. Seikh, E. S. M. Sherif, dan K. S. Nisar. "Stability Analysis and Multiple Solution of Cu-Al_2O_3/H_2O Nanofluid Contains Hybrid Nanomaterials Over a Shrinking Surface in the Presence of Viscous Dissipation." *Journal of Materials Research and Technology* 9, no. 1 (January 2020): 421–432. https://doi.org/10.1016/j.jmrt.2019.10.071

[49] Waini, I., A. Ishak, dan I. Pop. "Melting Heat Transfer of a Hybrid Nanofluid Flow Towards a Stagnation Point Region with Second-Order Slip." *Proceedings of the Institution of Mechanical Engineers, Part E: Journal of Process Mechanical Engineering* 235, no. 2 (April 2021): 405–415. https://doi.org/10.1177/0954408920961213

[50] Hamid, A., Hashim, M. Khan, dan A. Hafeez. "Unsteady Stagnation-Point Flow of Williamson Fluid Generated by Stretching/Shrinking Sheet with Ohmic Heating." *International Journal of Heat and Mass Transfer* 126 (November 2018): 933–940. https://doi.org/10.1016/j.ijheatmasstransfer.2018.06.110

[51] Khan, A. A., K. Zaimi, dan T. Y. Ying. "Stagnation Point Flow of Williamson Nanofluid Towards a Permeable Stretching/Shrinking Sheet with a Partial Slip." *CFD Letters* 12, no. 6 (2020): 39–56. https://doi.org/10.37934/cfdl.12.6.3956

[52] Khan, U., A. Zaib, S. A. Bakar, A. Ishak, D. Baleanu, dan E. S. M. Sherif. "Computational Simulation of Cross-Flow of Williamson Fluid Over a Porous Shrinking/Stretching Surface Comprising Hybrid Nanofluid and Thermal Radiation." *AIMS Mathematics* 7, no. 4 (2022): 6489–6515. https://doi.org/10.3934/math.2022362

[53] Zainal, N. A., R. Nazar, K. Naganthran, dan I. Pop. "Stability Analysis of MHD Hybrid Nanofluid Flow Over a Stretching/Shrinking Sheet with Quadratic Velocity." *Alexandria Engineering Journal* 60 (2021): 915–926. https://doi.org/10.3390/sym12020276

[54] Zainal, N. A., R. Nazar, K. Naganthran, dan I. Pop. "MHD Flow and Heat Transfer of Hybrid Nanofluid Over a Permeable Moving Surface in the Presence of Thermal Radiation." *International Journal of Numerical Methods for Heat and Fluid Flow* 31 (2021): 858–879. https://doi.org/10.1063/1.4944557

[55] Jamaludin, A., K. Naganthran, R. Nazar, dan I. Pop. "MHD Mixed Convection Stagnation-Point Flow of Cu-Al_2O_3/Water Hybrid Nanofluid Over a Permeable Stretching/Shrinking Surface with Heat Source/Sink." *European Journal of Mechanics, B/Fluids* 84 (2020): 71–80. https://doi.org/10.1615/HeatTransRes.2012005763

[56] Hussain, S., S. E. Ahmed, dan T. Akbar. "Entropy Generation Analysis in MHD Mixed Convection of Hybrid Nanofluid in an Open Cavity with a Horizontal Channel Containing an Adiabatic Obstacle." *International Journal of Heat and Mass Transfer* 114 (2017): 1054–66. https://doi.org/10.1016/j.ijheatmasstransfer.2017.06.135

[57] Khashi'ie, N. S., N. M. Arifin, dan I. Pop. "Magnetohydrodynamics (MHD) Boundary Layer Flow of Hybrid Nanofluid Over a Moving Plate with Joule Heating." *Alexandria Engineering Journal* 61 (2022): 1938–45. https://doi.org/10.1016/j.aej.2021.08.059

[58] Wahid, N. S., N. M. Arifin, N. S. Khashi'ie, I. Pop, N. Bachok, dan M. E. H. Hafidzuddin. "MHD Mixed Convection Flow of a Hybrid Nanofluid Past a Permeable Vertical Flat Plate with Thermal Radiation Effect." *Alexandria Engineering Journal* 61 (2022): 3323–33. https://doi.org/10.1016/j.aej.2021.08.059

[59] Wahid, N. S., N. M. Arifin, N. S. Khashi'ie, I. Pop, N. Bachok, dan E. H. Hafidzuddin. "MHD Hybrid Nanofluid Flow with Convective Heat Transfer Over a Permeable Stretching/Shrinking Surface with Radiation." *International Journal of Numerical Methods for Heat and Fluid Flow* 32 (2022): 1706–27. https://doi.org/10.1108/HFF-04-2021-0263

[60] Zainal, N. A., R. Nazar, K. Naganthran, dan I. Pop. "Unsteady MHD Stagnation Point Flow Induced by Exponentially Permeable Stretching/Shrinking Sheet of Hybrid Nanofluid." *Engineering Science and Technology, an International Journal* 24 (2021d): 1201–10. https://doi.org/10.1108/HFF-04-2021-0263

[61] Shateyi, S., dan H. Muzara. "On the Numerical Analysis of Unsteady MHD Boundary Layer Flow of Williamson Fluid Over a Stretching Sheet and Heat and Mass Transfers." *Computation* 8, no. 2 (June 2020). https://doi.org/10.3390/computation8020055

[62] Hussain, M., S. Jahan, Q. A. Ranjha, J. Ahmad, M. K. Jamil, dan A. Ali. "Suction/Blowing Impact on Magneto-Hydrodynamic Mixed Convection Flow of Williamson Fluid Through Stretching Porous Wedge with Viscous Dissipation and Internal Heat Generation/Absorption." *Results in Engineering* 16 (December 2022). https://doi.org/10.1016/j.rineng.2022.100709

[63] Almaneea, A. "Numerical Study on Heat and Mass Transport Enhancement in MHD Williamson Fluid via Hybrid Nanoparticles." *Alexandria Engineering Journal* 61, no. 10 (October 2022): 8343–54. https://doi.org/10.1016/j.aej.2022.01.041

[64] Yahya, Asmat Ullah, Sayed M. Eldin, Suleman H. Alfalqui, Rifaqat Ali, Nadeem Salamat, Imran Siddique, and Sohaib Abdal. "Computations for efficient thermal performance of Go+ AA7072 with engine oil based hybrid nanofluid transportation across a Riga wedge." *Heliyon* 9, no. 7 (2023). https://doi.org/10.1016/j.heliyon.2023.e17920

[65] Alkasasbeh, Hamzeh Taha, and Muhammad Khairul Anuar Mohamed. "MHD (SWCNTS+ MWCNTS)/H2O-based Williamson hybrid nanofluids flow past exponential shrinking sheet in porous medium." *FHMT.* 21, no. 1 (2023): 265-279. https://doi.org/10.32604/fhmt.2023.041539

[66] Ali, Farhan, Aurang Zaib, Mohamed Abbas, G. Anitha, K. Loganathan, and G. Ravindranath Reddy. "Radiative flow of cross ternary hybrid nanofluid (MoS2, TiO2, Ag/CMC-water) in a Darcy Forchheimer porous medium over a stretching cylinder with entropy minimization." *Heliyon* 10, no. 14 (2024). https://doi.org/10.1016/j.heliyon.2024.e34048

[67] Zainith, P., dan N.K. Mishra. "Experimental Investigations on Stability and Viscosity of Carboxymethyl Cellulose (CMC)-Based Non-Newtonian Nanofluids with Different Nanoparticles with the Combination of Distilled Water." *International Journal of Thermophysics* 42, no. 10 (2021): 137. https://doi.org/10.1007/s10765-021-02890-1

[68] Jain, Ruchi, Ruchika Mehta, Anurag Bhatnagar, Hijaz Ahmad, Zareen A. Khan, and Gamal M. Ismail. "Numerical study of heat and mass transfer of williamson hybrid nanofluid (CuO/CNT's-water) past a permeable stretching/shrinking surface with mixed convective boundary condition." *Case Studies in Thermal Engineering* 59 (2024): 104313. https://doi.org/10.1016/j.csite.2024.104313

[69] Aselebe, L. O., A. T. Adeosun, K. B. Kasali, B. M. Yisa, K. A. Salaudeen, and R. O. Adesina. "Investigation of thermal properties of ethylene glycol-based Williamson hybrid-nanofluid over stretchable/shrinking flat plate and their effects on solar panels." *International Journal of Thermofluids* 24 (2024): 100892. https://doi.org/10.1016/j.ijft.2024.100892

[70] Yashkun, U., K. Zaimi, A. Ishak, I. Pop, dan R. Sidaoui. "Hybrid Nanofluid Flow Through an Exponentially Stretching/Shrinking Sheet with Mixed Convection and Joule Heating." *International Journal of Numerical Methods for Heat and Fluid Flow* 31, no. 6 (2020): 1930–50. https://doi.org/10.1108/HFF-07-2020-0423

[71] Swalmeh, M.Z., F.A. Alwawi, M.S. Kausar, M.A.H. Ibrahim, A.S. Hamarsheh, I.M. Sulaiman, dan B. Panyanak. "Numerical Simulation on Energy Transfer Enhancement of a Williamson Ferrofluid Subjected to Thermal Radiation and a Magnetic Field Using Hybrid Ultrafine Particles." *Scientific Reports* 13, no. 1 (2023): 3176. https://doi.org/10.1038/s41598-023-29707-5

[72] Waini, I., A. Ishak, dan I. Pop. "MHD Flow and Heat Transfer of a Hybrid Nanofluid Past a Permeable Stretching/Shrinking Wedge." *Applied Mathematics and Mechanics* 41, no. 3 (2020): 507–20. https://doi.org/10.1007/s10483-020-2584-7